

Broadband Optical Phase Modulator with Low Residual Amplitude Modulation

Michael Nickerson*, Paul Verrinder, Lei Wang, Bowen Song, and Jonathan Klamkin
Department of Electrical and Computer Engineering, University of California, Santa Barbara, CA 93106, USA
*nickersonm@ece.ucsb.edu

Abstract: An optical phase modulator suitable for monolithic integration demonstrates efficient operation from 980 nm through 1360 nm. Measured $V_{\pi}L$ ranges from 0.6 V·cm to 1.22 V·cm with less than 0.5 dB residual amplitude modulation. © 2022 The Author(s)

1. Introduction

Integrated phase modulators are essential for many next-generation applications including telecommunications, LIDAR, and machine learning [1], [2]. However, the common silicon photonics platform only supports slow thermal phase modulators and absorption modulators with high residual amplitude modulation (RAM). Integration of other materials such as lithium niobate can provide fast and low-loss modulators, but significantly increases complexity. Silicon photonics also lacks integrated lasers, and is limited to wavelengths above 1100 nm, excluding the region near 1000 nm that is commonly utilized for applications such as topographical and remote-sensing LIDAR. In contrast, group III-V semiconductor platforms offer on-chip lasers, optical gain, and efficient phase modulators at a variety of wavelengths from 780nm through 2000nm.

This work presents gallium arsenide (GaAs) phase modulators with low fabrication complexity that are suitable for use in monolithic photonic integrated circuits, which may include GaAs-based laser sources in the 1000-1300 nm range [3], [4] for applications such as optical phased arrays [5]. Measured from 980 nm through 1360 nm, these modulators demonstrate single-sided $V_{\pi}L$ of 0.6 V·cm to 1.22 V·cm and RAM below 0.5 dB for more than 2π phase shift. Tested wavelengths are equipment-limited, and functionality is expected outside of this wavelength range.

2. Device Design and Fabrication

The modulator epitaxy was developed as a reverse-biased P-p-i-n-N double heterostructure to reduce RAM and propagation loss. The design yields high overlap between a nearly linear electric field and the optical mode to utilize the strong linear and quadratic electro-optic effects in GaAs, as shown in Figure 1(a). Low optical absorption is achieved by a graded-index structure providing 94% overlap between the optical field and the GaAs guiding region and 10% overlap with free carriers.

Modulators were implemented as deep ridge waveguides formed by a Cl_2/N_2 ICP etch, with P-contacts deposited on top and N-contacts placed nearby on the highly n-doped GaAs buffer layer (Fig. 1(b)). Passive waveguides for edge coupling simply omit the metal contacts (Fig. 1(c)).

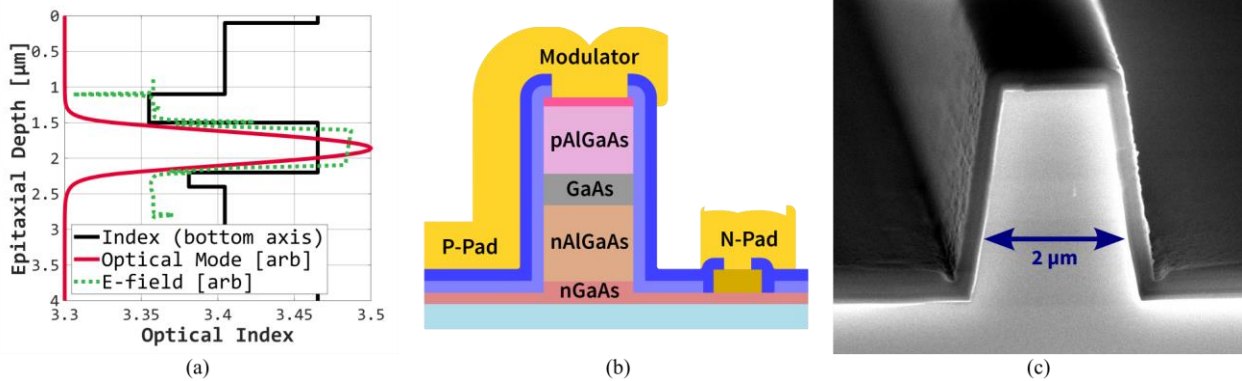


Figure 1. (a) Simulated 1D optical mode and electric field. (b) Cross-section schematic of modulator waveguide. (c) SEM image of fabricated passive waveguide edge coupler; scale approximately corresponds to the cross-section schematic.

3. Measurement Results

Devices were characterized by edge coupling to lensed fibers. Packaged 980 nm and 1030 nm DFB lasers and a tunable O-band laser were used as light sources. The modulation response of 4 mm devices was determined by simultaneously fitting multiple single-sided Mach-Zehnder modulator (MZM) transmission measurements, and separately by

Fabry-Perot waveguide cavity fringes [6]. Tested across a range of wavelengths from 980 nm to 1360 nm, these devices demonstrated single-sided $V_{\pi} \cdot L$ ranging from 0.6 V·cm to 1.22 V·cm for the TE optical mode (Fig. 2(a)).

Modulator RAM was characterized by MZM fringe peaks and is under 0.5 dB until the onset of Franz-Keldysh electroabsorption, reaching 3 dB at a reverse bias of 5.5 V at 980 nm, 12 V at 1030 nm, and equipment-limited >15 V above 1260 nm. DC leakage currents as small as 50 nA at -5 V bias corresponds to DC power usage under 200 nW per modulator for $>2\pi$ modulation at 980 nm and 1030 nm. Response bandwidth was not measured above 1 MHz, but electrical testing determined 7 pF combined junction and parasitic capacitance and 10 Ω series resistance.

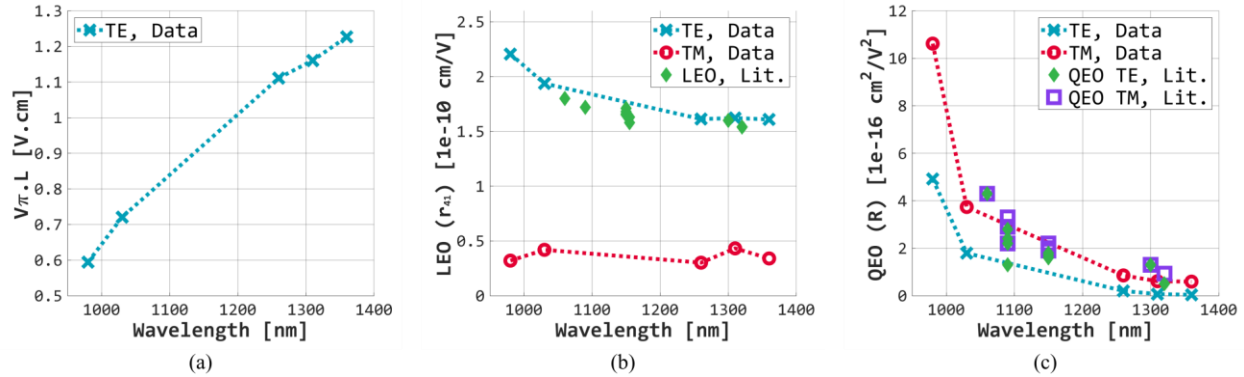


Figure 2. (a) Measured TE-mode efficiency of 4 mm modulator. (b) Measured linear modulation efficiency and expected electro-optic coefficients from literature. (c) Measured quadratic modulation efficiency and expected electro-optic coefficients from literature.

Casting quadratically-fit modulation efficiency to linear and quadratic electro-optic coefficients, the measured performance agrees well with known GaAs values from literature (Fig. 2(b,c)) [7]–[9]. This comparison relies on simulated values for the electrical field in the optical guiding layer, and roughly agrees with a simple assumption of applying the bias voltage directly across the p-i-n GaAs layers. The nonzero linear terms for TM polarization are attributed to uncharacterized carrier effects and imperfect polarization, which was not rigorously controlled. The depressed TE quadratic coefficient is under further investigation.

4. Conclusion

A GaAs-based optical phase modulator has been demonstrated with measured single-sided $V_{\pi} \cdot L$ modulation efficiency ranging from 0.6 V·cm at 980 nm to 1.22 V·cm at 1360 nm. RAM is less than 0.5 dB for more than 2π modulation at all tested wavelengths. Fabricated as a deep ridge waveguide modulator including passive routing for edge coupling, the design is ideal for use in monolithic GaAs-based photonic integrated circuits, with broad applicability including optical phased arrays with on-chip lasers.

5. Acknowledgements

The authors thank Jim Brookhyser, Gregory Erwin, and Jan Kleinert for useful discussions, and acknowledge funding support from MKS Instruments. A portion of this work was performed in the UCSB Nanofabrication Facility.

6. References

- [1] B. J. Shastri *et al.*, “Photonics for artificial intelligence and neuromorphic computing,” *Nature Photonics*, vol. 15, pp. 102–114, Feb. 2021. <https://doi.org/10.1038/s41566-020-00754-y>
- [2] C. Doerr, “Silicon photonic integration in telecommunications,” *Frontiers in Physics*, vol. 3, 2015. <https://doi.org/10.3389/fphy.2015.00037>
- [3] P. A. Verrinder *et al.*, “Gallium Arsenide Photonic Integrated Circuit Platform for Tunable Laser Applications,” *IEEE Journal of Selected Topics in Quantum Electronics*, vol. 28, pp. 1–9, Jan. 2022. <https://doi.org/10/gmzfnn>
- [4] L. Wang *et al.*, “High Performance 1.3 μ m Aluminum-Free Quantum Dot Lasers Grown by MOCVD,” *2020 Optical Fiber Communications Conference and Exhibition (OFC)*, Mar. 2020, pp. 1–3.
- [5] M. Nickerson *et al.*, “Broadband and Low Residual Amplitude Modulation Phase Modulator Arrays for Optical Beamsteering Applications,” *2022 Conference on Lasers and Electro-Optics (CLEO)*, to be published.
- [6] R. Regener and W. Sohler, “Loss in low-finesse Ti:LiNbO₃ optical waveguide resonators,” *Applied Physics B*, vol. 36, no. 3, pp. 143–147, Mar. 1985. <https://doi.org/10/b9h5xb>
- [7] J. Faist and F. -K. Reinhart, “Phase modulation in GaAs/AlGaAs double heterostructures. II. Experiment,” *Journal of Applied Physics*, vol. 67, no. 11, pp. 7006–7012, Jun. 1990. <https://doi.org/10/cj4hq7>
- [8] C. A. Berseth, C. Wuethrich, and F. K. Reinhart, “The electro-optic coefficients of GaAs: Measurements at 1.32 and 1.52 μ m and study of their dispersion between 0.9 and 10 μ m,” *Journal of Applied Physics*, vol. 71, no. 6, pp. 2821–2825, Mar. 1992. <https://doi.org/10/ctg32h>
- [9] S. S. Lee, R. V. Ramaswamy, and V. S. Sundaram, “Analysis and design of high-speed high-efficiency GaAs-AlGaAs double-heterostructure waveguide phase modulator,” *IEEE Journal of Quantum Electronics*, vol. 27, no. 3, pp. 726–736, Mar. 1991. <https://doi.org/10/bhd2dh>